

# An Evaluative Tool For Preoperative Planning of Brain Tumor Resection

Aaron M. Coffey<sup>1</sup>, Ishita Garg<sup>1</sup>, Michael I. Miga<sup>1</sup>, Reid C. Thompson<sup>2</sup>

<sup>1</sup> Vanderbilt University, Dept. of Biomedical Engineering, P.O. 1631, Station B, Nashville, TN, USA

<sup>2</sup> Vanderbilt University Medical Center, Department of Neurological Surgery, T-4224MCN/VUMC

## ABSTRACT

A patient specific finite element biphasic brain model has been utilized to codify a surgeon's experience by establishing quantifiable biomechanical measures to score orientations for optimal planning of brain tumor resection. When faced with evaluating several potential approaches to tumor removal during preoperative planning, the goal of this work is to facilitate the surgeon's selection of a patient head orientation such that tumor presentation and resection is assisted via favorable brain shift conditions rather than trying to allay confounding ones. Displacement-based measures consisting of area classification of the brain surface shifting in the craniotomy region and lateral displacement of the tumor center relative to an approach vector defined by the surgeon were calculated over a range of orientations and used to form an objective function. The objective function was used in conjunction with Levenberg-Marquardt optimization to find the ideal patient orientation. For a frontal lobe tumor presentation the model predicts an ideal orientation that indicates the patient should be placed in a lateral decubitus position on the side contralateral to the tumor in order to minimize unfavorable brain shift.

**Keywords:** Brain shift, patient positioning, tumor resection, finite elements

## 1. INTRODUCTION

Neurological procedures involving the resection of brain tumors require the surgeon to evaluate the most desirable approach for extraction, one which facilitates tumor access and removal while minimizing damage to surrounding healthy tissue. Intraoperative brain shift complicates this evaluation. Studies in the literature have reported non-rigid deformation of a centimeter or more<sup>[1]</sup> during surgery owing to a variety of reasons such as administration of hyperosmotic drugs, edema, gravity, pathology, respiration, and surgical manipulation.<sup>[2,3,4]</sup> The shift causes concerns with the conformance of the visual presentation of the brain to the preoperative tomograms being used for image guidance. This compromise of the spatial relationship between physical space in the operating room (OR) and the patient's preoperative image tomograms in the context of image-guided surgery suggests that an evaluation tool for minimizing shift might be used to reduce the discrepancy between the two.

Besides issues with image guidance, brain shift also frequently requires the usage of retractors to obtain favorable access to the tumor. The resultant retraction forces potentially damage healthy tissue. To mitigate the possible consequences of applying retraction, one possible approach is to orient the patient to where gravity and other shift mechanisms generate a favorable brain shift such that the use of retraction is minimized. Towards this end, analysis of the underlying patient positioning criteria used by our participating surgeon has suggested a series of biomechanical measures that form a basis upon which to optimize model-based selection of patient orientation in the following work.

In previous work Kevin Ha et al.<sup>[5]</sup> demonstrated increased mid-line tumor accessibility for tumors in close proximity to the falx cerebri based upon tumor stress criteria. The position-dependent gravitationally induced tensile stresses on the tumor surface pulling the surrounding brain tissue away from the tumor was found to allow easier resection and reduced

likelihood for the need for retraction. However, this enhanced tumor exposure was noted to come at the expense of greater intraoperative shift. The following work examines a large frontal lobe tumor in the context of shift minimization to demonstrate a possible solution to the nontrivial task of patient positioning for surgery.

## 2. METHODS

### 2.1 Computational model

A 3D finite element computational brain model based upon Biot's theory of soil consolidation<sup>[8]</sup> was used to simulate brain shift under varying conditions. Biot's consolidation theory describes the mechanical behavior of a poroelastic medium<sup>1</sup> using a linearly elastic description of the solid matrix and Darcy's law for fluid flow through the porous matrix. Deformations can be caused by surface forces, displacements, interstitial fluid pressure gradients, or changes to tissue buoyancy. Changes in the volumetric strain rate depend upon the interstitial pressure and hydration. The usage of this biphasic model for simulating the soft tissue mechanics associated with brain shift is well established in the literature.<sup>[4,6,7,9,10,11,12,13]</sup> This particular model has been previously validated for performing model-updated image guided surgery in phantom, animal, and human studies.<sup>[4,6,7,9,10,11]</sup>

$$\nabla \cdot G \nabla \bar{u} + \nabla \frac{G}{1-2\nu} (\nabla \cdot \bar{u}) - \alpha \nabla p = -(\rho_t - \rho_f) g \quad (1)$$

$$\alpha \frac{\partial}{\partial t} (\nabla \cdot \bar{u}) + \frac{1}{S} \frac{\partial p}{\partial t} + k_c (p - p_c) = \nabla \cdot k \nabla p \quad (2)$$

In equation (1) and (2),  $u$  is the displacement vector,  $p$  the interstitial pressure,  $G$  the shear modulus,  $\nu$  is Poisson's ratio,  $\alpha$  the ratio of fluid volume extracted to volume change of the tissue under compression,  $\rho_t$  the tissue density,  $\rho_f$  the fluid density,  $g$  the gravitational unit vector,  $t$  the time,  $1/S$  the amount of fluid which can be forced into the tissue under constant volume,  $k_c$  the capillary permeability,  $p_c$  the intracapillary pressure, and  $k$  the hydraulic conductivity. The right hand side term in equation (1) describes the effect of gravitational forces on the brain as a difference in density between tissue and surrounding fluid. Intraoperative drainage of CSF reduces the buoyancy forces counteracting gravity thereby resulting in the brain sagging due to gravitational forces. Hyperosmotic drugs such as mannitol, which reverse the blood-brain osmotic barrier, reduce the volume of the brain by drawing water from the extracellular spaces. The third term in equation (2) is used to model these drug effects. The model is capable of simulating effects from hyperosmotic drugs, gravity-induced deformation, retraction, resection, and swelling from edema.<sup>[7,9,12]</sup> With finite element treatment, the partial differential equations in (1) and (2) are solved numerically using the Galerkin weighted residual method coupled with a weighted time stepping scheme.<sup>[7,14,15]</sup>

### 2.2 Model and boundary condition generation

Observation within the OR of the surgical planning phase suggests that the surgeon defines an 'approach' vector to the tumor via use of an image-guidance system. This vector is the line that extends from the center of the tumor to a point on the scalp the surgeon notes the tumor lies directly under with a guidance probe. Upon exposure of the skull, this point is again marked, indicating it is a significant landmark, and typically lies in the center of the chosen craniotomy. This important vector is used within this work for resection of the brain mesh and for determining the quantitative measures. For the clinical case being analyzed, it was approximated as the normal to the craniotomy region created by averaging all the node normals within the craniotomy.

Generation of a patient-specific brain model utilizes pre-surgical planning and data realized by the surgeon. The brain and tumor surfaces are first segmented manually from a gadolinium-enhanced tomographic image volume. A tetrahedral mesh of approximately 120,000 elements is then created using these surfaces and the material types of the mesh elements are classified as gray or white matter according to gray scale thresholds applied to the image volume via an

<sup>1</sup> A medium consisting of a solid matrix containing connected pores filled with a fluid

image-to-grid method.<sup>[15,16]</sup> The brain surface surrounding the craniotomy and the tumor surface are refined such that the characteristic length of a boundary element is half that elsewhere. A patient specific falx cerebri membrane is inserted by splitting the mesh and applying special boundary conditions-- no displacement across the falx but the brain and falx are allowed to slip along the cranial wall. The elements classified as tumor are removed via a resection element list which decouples the respective equilibrium equation. Additionally, a cylindrical plug of tissue from tumor center to brain surface with axis being the 'approach' vector and of radius 70% of the average tumor radius is removed from the mesh to allow relaxation into the resultant resection cavity. All elements with centroid coordinates within the radius as determined by a distance from a point to a line test are added to the resection element list. The tumor surface and cylinder surfaces combined define the resection cavity which is specified to be stress-free and at atmospheric pressure.

As the mesh is rotated for each orientation in a condition set, an automatic boundary condition generator<sup>[7]</sup> classifies the nodes on the brain surface as fixed, allowed to slip along tangent-to-the brain surface, or stress-free according to the varying orientation. Two modifications were made to the generator by Dumpuri et al.<sup>[7]</sup> First, as a consequence of manual optimization of a model to the clinical data, the mean height of those brain surface nodes whose dot products with the gravity vector lay between -0.2 and -0.4 was used as the stress-free level as a better shift recovery<sup>[7]</sup> resulted. Second, the cerebrospinal fluid (CSF) drainage level is specified such that in each orientation one third of the volume of the brain is submerged as determined by summing the volumes of the submerged elements. Maintaining this fraction across orientations also results in keeping the change in tissue buoyancy force causing brain sag the same across orientations. Craniotomy region placement on the mesh is established via determining which brain surface boundary elements lay within the perimeter of the pre-resection laser range scan cortical surface area defined as the craniotomy using the approach vector as the line of sight.

The nodes composing the elements in the resection list are decoupled from the biphasic model analogous to the removal of its tissue counterpart. The decoupled nodes lack displacement solutions. This includes the node at the tumor center whose displacement is used as a measure. Reconstruction of the solutions for the resected nodes is therefore required. This reconstruction is achieved by using a linear elastic model after obtaining displacements on every node on the resection cavity surface for the boundary conditions. The only missing displacements in the output of the biphasic model are those on the nodes inside the resection hole on the brain surface. They are obtained from thin-plate spline interpolation using nodes within 1.25cm of the hole perimeter as control points. The linear elastic model output is combined with the biphasic model's output to yield a complete volumetric displacement description of the brain from which the shift measures can be derived.

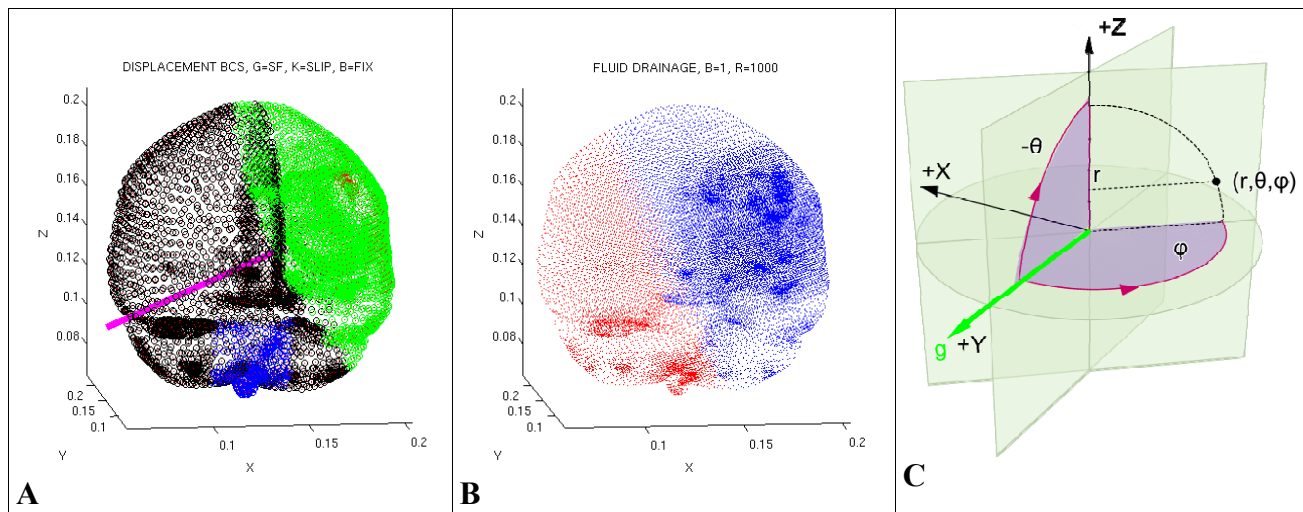


**Figure 1:** (A) Representative boundary condition set where green nodes are stress-free (free to deform), black are slip nodes (no movement in the normal direction), blue nodes are fixed, magenta gravity vector indicated. (B) Corresponding CSF drainage level where red are submerged (no drainage) and blue are at atmospheric pressure. (C) Spherical coordinate system for head orientations with neutral gravity  $g = [0 \ 1 \ 0]$  defined to be  $\phi = 0^\circ$ ,  $\theta = 0^\circ$ , i.e.  $[0^\circ \ 0^\circ]$ .

### 2.3 Derived measures

Using the falx membrane as a support to reduce shift, the neurosurgeon seeks to orient the patient so that gravity-induced shift aids tumor resection. This shift minimization strategy suggested using displacement-based metrics such as lateral shift of the tumor center as viewed along the line of sight established by the ‘approach’ vector and minimization of change to the field of view in the craniotomy. The tumor center is defined as the node closest to the volumetric centroid of the tumor elements. The lateral displacement is the perpendicular component of the tumor center's displacement to the ‘approach’ vector. The change to the field of view was quantified by classifying the brain surface area within the craniotomy using the ‘approach’ vector as the line of sight. To get a finer resolution of the area contained in the craniotomy, the brain surface is first post-processed by splitting each boundary element into four using extra nodes at the midpoints of each segment to create extra boundary elements. Then the perimeter of the craniotomy in conjunction with the boundary element centroid coordinates is used in a standard point inside a polygon test to segment the brain surface into elements inside and outside the craniotomy. This segmentation defines an area map. An area map of the boundary elements before deformation is used to delineate the original craniotomy surface. After deformation an area map recording those boundary elements within the craniotomy perimeter is again created. Boundary elements common to both maps are classified as area staying visually the same. Boundary elements visible in the pre-deformation map but not in the post-deformation map are classified as area leaving the craniotomy. Boundary elements visible in the post- map but not in the pre- map become area entering the craniotomy.

### 2.4 Laser range scan area classification

Laser range scan (LRS) clinical data is used to classify cortical surface area within the field of view of the craniotomy for measuring surface shift and to establish the intraoperative displacements of selected points. The first step in obtaining these measurements is to fit a pre-resection LRS and post-resection LRS with texture-mapped radial basis function (RBF) surfaces. These surfaces are segmented to produce a craniotomy of equal area and shape. Homologous points on the pre- LRS surface and post- LRS surface are identified at the intersection of corresponding vessels. These serve as control points for a thin-plate spline transformation warping the pre- LRS surface to the post- surface to create a combined surface. The combined surface is segmented to find the area entering and leaving the craniotomy on a clinical basis against which to evaluate the model results in terms of quantity and distribution. The pre/post change in coordinates of the homologous points also defines known brain shift displacements to match with a model.

### 2.5 Objective function and optimization

An objective function (OF) in the context of least squares minimization is used to evaluate a range of orientations of the patient. Minimization of the lateral displacement would result in the desirable behavior of the tumor center remaining directly beneath the specified point by the surgeon. Minimization of the area leaving the craniotomy promotes maintaining the surgical field of view and proportionately indicates a favorable reduction in surface shift. The objective function is written as

$$G(\varphi, \theta) = \min \left\{ \lambda_1 \|A - A_0\|^2 + \lambda_2 \|\vec{\delta}\|^2 \right\} \quad (3)$$

where  $A$  is the defined craniotomy area and  $A_0$  the area that remains visually the same such that  $A - A_0$  represents the area leaving the craniotomy and  $\vec{\delta} = [\delta_x, \delta_y, \delta_z]$  are the tumor center lateral displacement x-, y-, and z- components respectively. Being of dissimilar order of magnitude, the measures require scaling so that one will not be unduly emphasized over another when optimal orientation is determined by a gradient descent method. The measures also require weighting for relative importance. Hence,  $\lambda_i = W_i S_i$  where  $W_i$  is the measure weight and  $S_i$  is the measure scaling parameter multiplies each term in the objective function. The scaling parameters  $S_i$  are the inverse of the variance of each respective measure within an atlas of orientations. The area and lateral displacement measures were equally weighted for importance.

The Levenberg-Marquardt (LM) optimization method was used to find the optimal patient orientation using the objective function defined in equation (3). The purpose was to determine how close it could come to the true minimum in the atlas in order to investigate the feasibility of dynamically optimizing the orientation from an initial starting orientation and potentially reduce the number of orientation evaluations needed in an atlas to find the minimum objective function value. The derivatives of the objective function within the Jacobian were computed via backward finite differences. For the LM method, the regularization value  $\lambda = 1e-10$  was used and optimization was terminated when the absolute difference in objective function evaluations between successive orientations achieved a tolerance of  $1e-5$ .

## 2.6 Material properties

The material properties for the model in Table 1 conform to those used by Dumpuri et al.<sup>[7]</sup> with the alteration of the  $k_c$  value for gray and white matter being made the same value.

Symbol	Value	Units
$E_{\text{white and gray}}$	2100	N/m <sup>2</sup>
$\nu$	0.45	unitless
$\rho_t$	1000	kg/m <sup>3</sup>
$\rho_f$	1000	kg/m <sup>3</sup>
$g$	9.81	m/s <sup>2</sup>
$\alpha$	1	unitless
$1/S$	0	unitless
$k_{\text{white}}$	$1 \times 10^{-10}$	m <sup>3</sup> s/kg
$k_{\text{gray}}$	$5 \times 10^{-12}$	m <sup>3</sup> s/kg
$k_{c,\text{white and gray}}$	$5.50 \times 10^{-9}$	Pa/s
$p_{c,\text{mannitol}}$	-3633	Pa

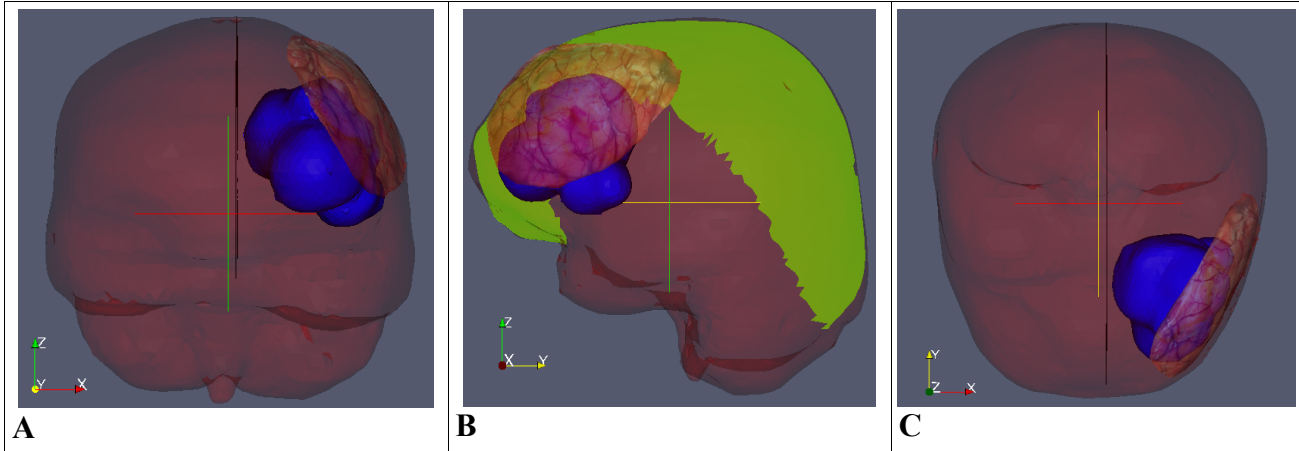
**Table 1:** Material properties used in the model

## 3. RESULTS

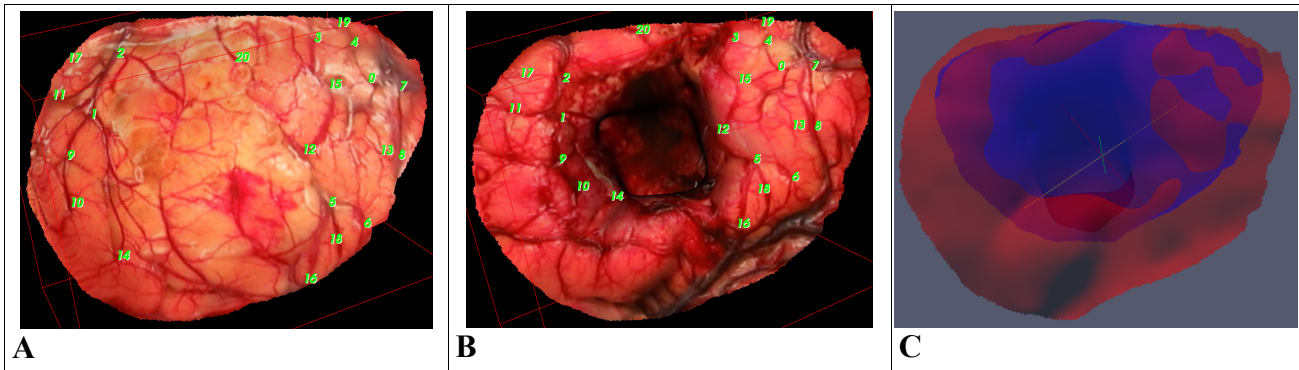
A clinical case involving a large frontal lobe tumor in the left hemisphere was analyzed. The three orthoviews in Figure 2 show the details of the location and shape of the patient specific falx, the location and extent of the craniotomy used, and the size and position of the tumor within the brain. Involving much of the volume of the left frontal lobe, the tumor had a volume of 63.61 cm<sup>3</sup> and an average radius of 2.48 cm. In Figure 3 the homologous points on the pre LRS and post LRS surfaces are identified. The distribution of the points around the edges of the craniotomy, surrounding the resection hole, and close to the hole's edge was chosen to provide a good selection of control points for warping the pre LRS surface to the post. The overlay is seen in Figure 3C. Good vessel correspondence especially around the edges of the deformed pre LRS surface on the post surface was observed. The displacements of the homologous points resulting from the surgeon's chosen orientation for the case were established and the best fit of a model sought. Manual optimization of the model parameters yielded a match of the model's displacements to those resulting from the surgical orientation with a shift recovery<sup>[7]</sup> of 67.90% which was in the range of the 70% to 80% reported in the literature. With the model parameters for producing the best match to the data established, an atlas of orientations was created wherein the model combined the effects of both gravity and mannitol.

For the atlas creation a spherical coordinate system for specifying orientations was used. The origin was defined to be the orientation where the default gravity vector lay along the axis from the frontal to the occipital lobe (the +y axis in Cartesian coordinates) with spherical rotation angles phi and theta of [0° 0°]. This orientation corresponded to the patient

laying supine. The atlas consisted of 504 orientations with the head being rotated in phi every 6 degrees from  $-16^\circ$  to  $146^\circ$  and tilted in theta every 8 degrees from  $-56^\circ$  to  $80^\circ$ . This range of orientations was chosen to guarantee finding the minimal value of the objective function.

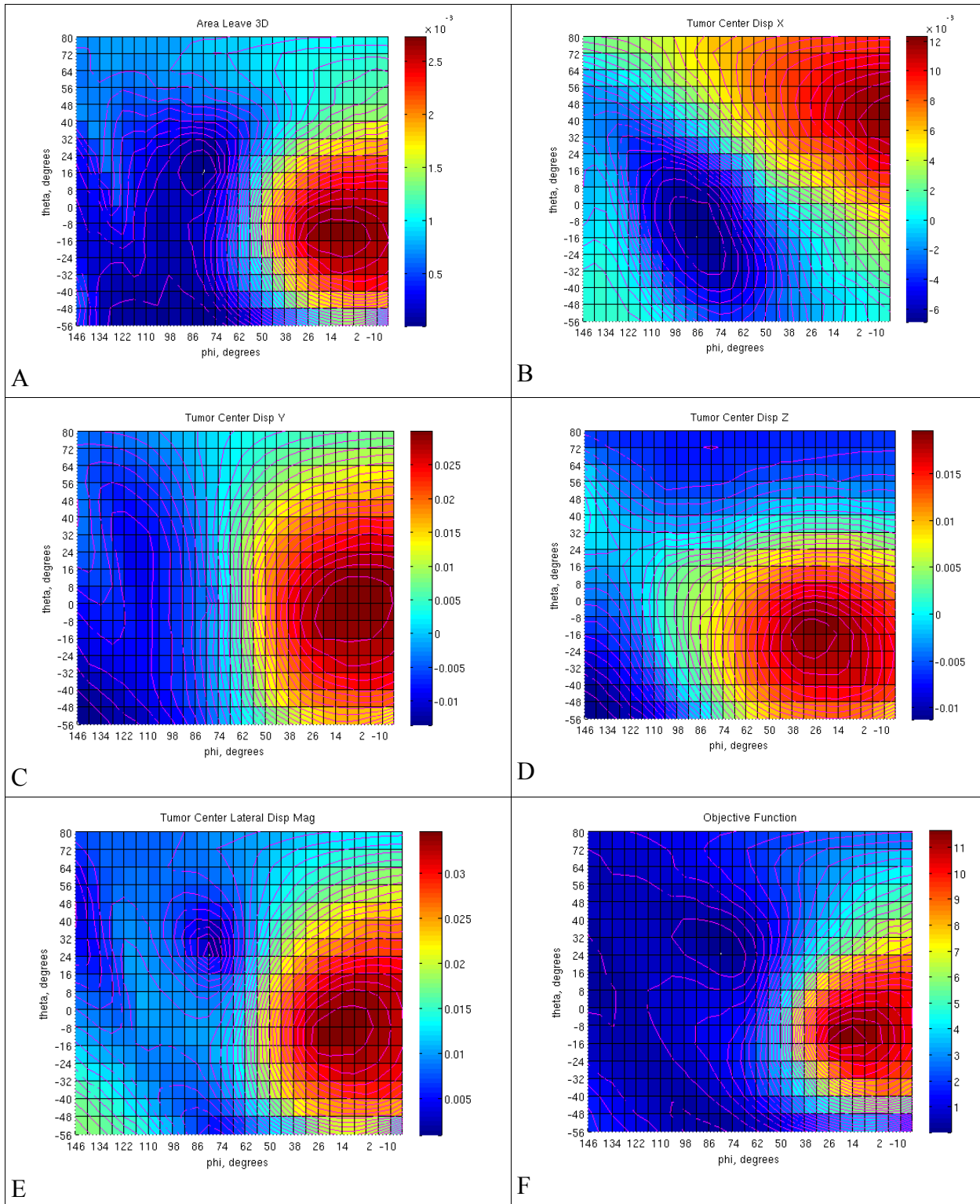


**Figure 2:** Three views of clinical case tumor presentation where brain surface is red, falx is green, tumor is blue, and the craniotomy from a LRS scan is indicated: (A) coronal view (B) sagittal view (C) transverse view



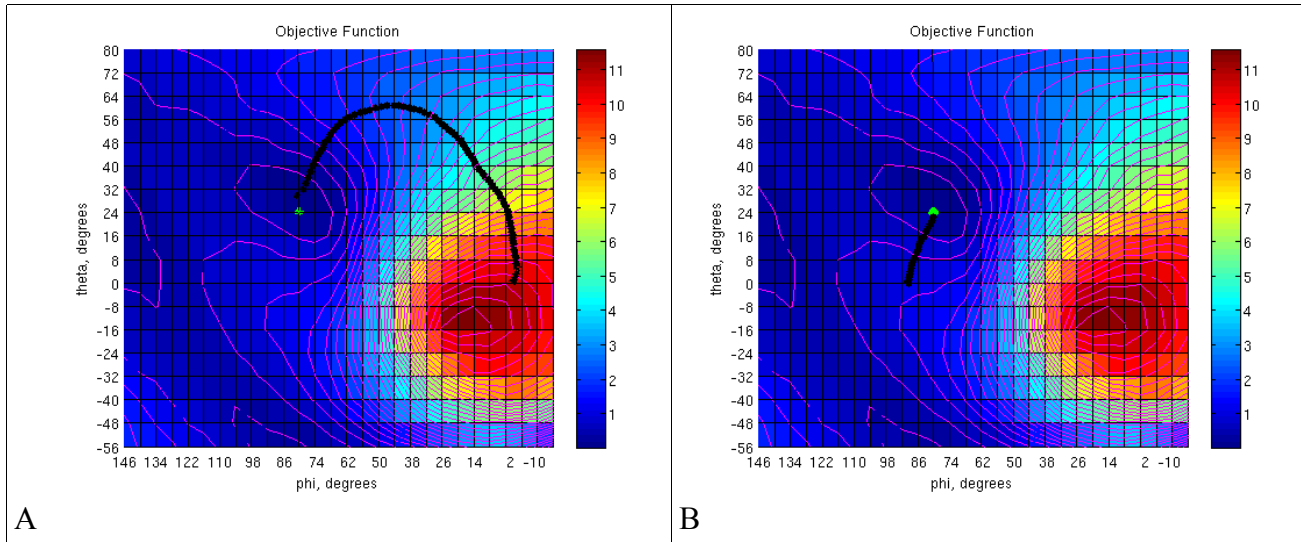
**Figure 3:** (A) 21 points selected on the pre-LRS surface (B) 21 homologous points on the post-LRS surface (C) the pre-LRS surface (blue) warped via a thin-plate spline transformation using the 21 control points to the post-LRS surface (red)

Figure 4 represents the calculation of the measures over the atlas of orientations. Area leaving the craniotomy was within the range  $[0, 2.724]$   $\text{cm}^2$ . The tumor center lateral displacement x- component ranged  $[-6.86, 12.29]$  mm, the y- displacement  $[-13.58, 29.94]$  mm, and the z- displacement  $[-11.28, 19.54]$  mm. The magnitude of the lateral displacement was within  $[0.99, 34.53]$  mm. Orientations where  $\phi > 104^\circ$  or  $\theta < -16^\circ$  amounted to over-rotation of the head such that the craniotomy region left the stress-free zone in the boundary condition set and hence were invalid. Discounting of these invalid orientations did not alter the orientation reported as being optimal as determined by the modeling.



**Figure 4:** Plots of measures over range of orientations and objective function. (A) Area leaving craniotomy area [ $\text{cm}^2$ ] (B) tumor center lateral displacement x- component [m] (C) tumor center lateral displacement y- component [m] (D) tumor center lateral displacement z- component [m] (E) tumor center lateral displacement magnitude [m] (E) objective function

Figure 5 presents the optimization path follow by the LM method. Two initial starting poses were used to examine the convergence to the final position, the supine position  $[0^\circ 0^\circ]$  and the lateral decubitus  $[90^\circ 0^\circ]$  with the tumor contralateral to the patient bed. The black markers indicate the sequence of orientations followed down the gradient with the optimal orientation achieved shown as a green marker. In Table 2 the best atlas result is the orientation with the minimum value of the objective function in the atlas. The best shift recovery orientation was the orientation where the model displacements on the nodes corresponding to the 21 LRS surface displacements achieved the highest value of shift recovery for the surgical orientation. The final orientation angles as reported by the LM method from the two poses are also recorded in Table 2.



**Figure 5:** Optimization pathways shown on the objective function from two initial positions. Black dots are previous orientations and the green dot marks the final orientation. (A) supine orientation  $[0^\circ 0^\circ]$  (B) lateral decubitus orientation  $[90^\circ 0^\circ]$ .

Orientation	Final Phi	Final Theta
Supine	$79.92^\circ$	$24.36^\circ$
Lateral Decubitus	$79.99^\circ$	$24.01^\circ$
Best Atlas Result	$80.00^\circ$	$24.00^\circ$
Best Shift Recovery	$66.30^\circ$	$-7.01^\circ$

**Table 2:** Optimal orientations with spherical rotation angles specified

Figure 6 and Table 3 display for visual and quantitative comparison the results of the optimization process seen in Figure 5. Figure 6A shows the area distribution according to the classification of the pre/post overlay of the clinical data. In Figure 6B-D the location of the tumor center before deformation within the craniotomy is shown by the magenta marker and its location after deformation by the green marker. Table 3 records the magnitude of the lateral shift of the tumor center as seen in Figure 6 and the area quantities. The orientation for the supine position in Figure 6C in phi and theta is the default:  $[0^\circ, 0^\circ]$ . The orientation in Figure 6B for best shift recovery is at  $[66.30^\circ, -7.01^\circ]$ . The orientation in Figure 6D for the model optimization has the angles  $[80^\circ, 24^\circ]$ .

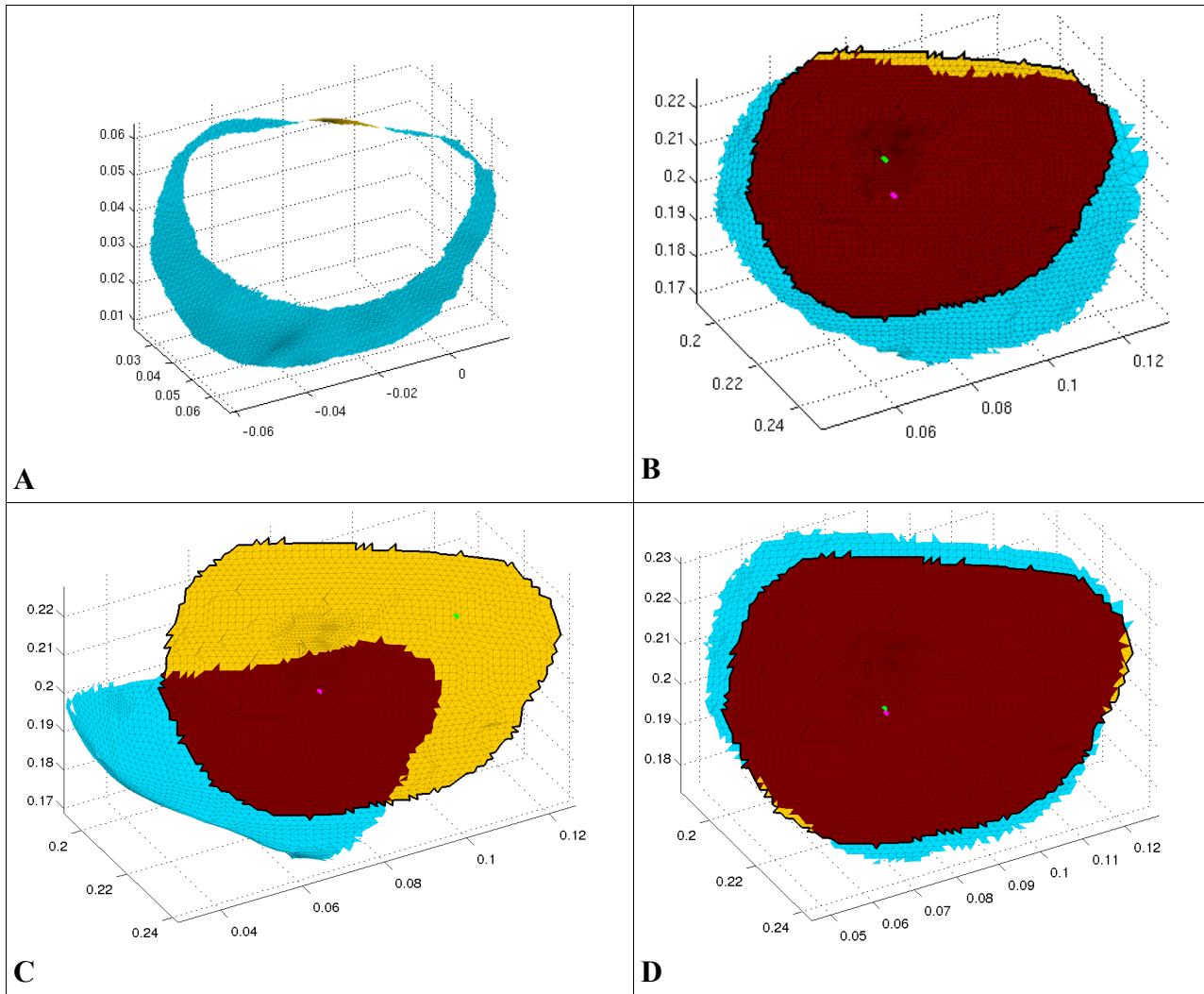


**Figure 6:** Blue boundary elements represent area entering, yellow leaving and red those that remain the same for the craniotomy. The magenta marker is the tumor center projected to the view plane of the craniotomy, and the green the displaced tumor center. (A) Area classification of LRS mapping (B) best shift correction orientation (C) supine orientation (D) model optimized orientation

Measure	Units	LRS	Best Shift	Supine	Model Optimized
Area Enter	cm <sup>2</sup>	17.29	17.07	15.61	8.45
Area Leave	cm <sup>2</sup>	0.13	1.70	25.51	0.41
Area Same	cm <sup>2</sup>	42.14	42.00	18.19	43.29
Craniotomy Area	cm <sup>2</sup>	42.27	43.70	43.70	43.70
Lateral Shift	mm	N/A	8.45	33.49	0.99

**Table 3:** Results for the measures for the four orientations

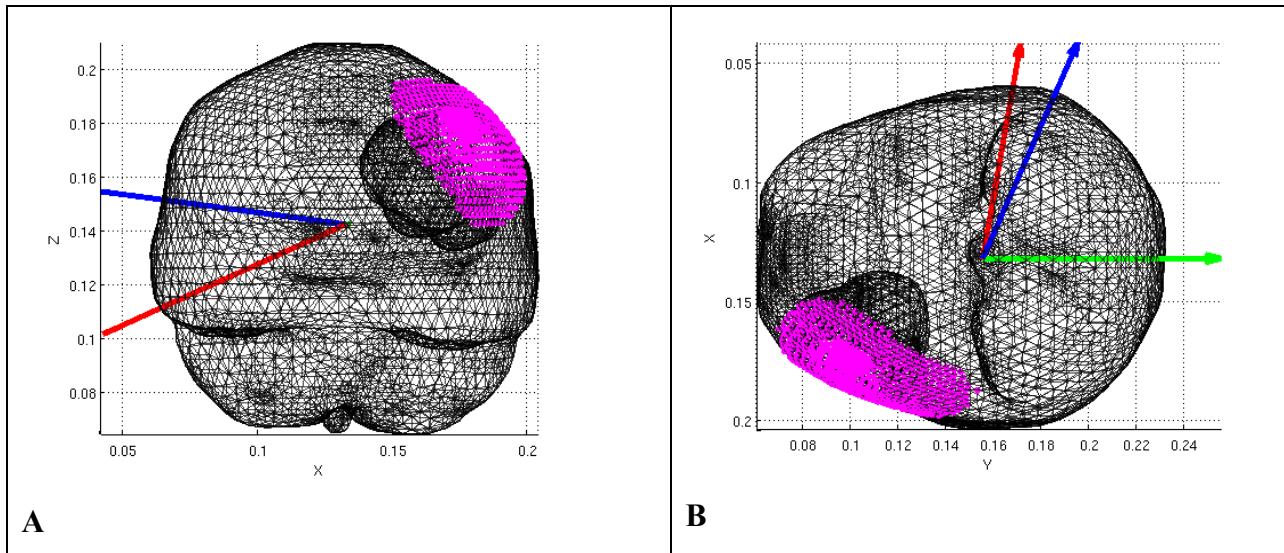


**Figure 7:** Comparison of best shift recovery orientation, optimized model orientation, and supine orientation sag vectors. Magenta region indicates the craniotomy, green is the supine sag vector, blue the shift recovery vector, and red the optimized model vector. (A) A coronal view looking at the frontal lobes foremost (B) Transverse view looking at top of head foremost

Figure 7 illustrates the differences in applied gravity vectors in the direction of which the brain sags for the standard supine, the best shift recovery match, and the model optimized orientations. Both the best shift recovery orientation and the optimized model orientation result in the craniotomy laying entirely within the stress-free region in the boundary condition set.

#### 4. DISCUSSION

Comparison of Figure 6A and 6B, or the fit of the model to the LRS data for the surgical orientation, shows a reasonable correspondence of areal distribution for a shift recovery of 67.90%. Better correspondence of the displacements—i.e. higher shift recovery— would result in area maps more closely approximating that seen in the clinical data and methods of achieving this improvement should be investigated. The area leaving amounts to 0.3% of the craniotomy area for the LRS data and 3.9% for the best shift recovery orientation and it occurs in the same region of the craniotomy for the shift recovery orientation as in the LRS mapping. The areas remaining the same within the craniotomy and entering the craniotomy agree well per Table 3, and the absolute error of the area leaving is small. As can be seen visually in Figure 5 and in the tabulation in Table 2, the optimization converges to an orientation very close to the global optimum. This orientation is successfully achieved from two initial poses, the supine position which is standard for frontal lobe tumors and from the lateral decubitus position. One should note, however, the susceptibility of the LM method to finding local minima, although in this clinical case the atlas global minimum was successfully found. The angular resolution of the atlas is fairly coarse which results in smoothing of the data. This smoothing may have contributed to the successful usage of the LM method by eliminating local minima in which the optimization process might have prematurely terminated.

Previous experiences in the OR have shown that in tumor resection cases where it is desirable to minimize shift the patient is placed by the surgeon in a lateral decubitus position on the side contralateral to the tumor. This position is shown to indeed have the advantage of reducing the anterior-posterior shift, as seen in Figure 6C and quantified in Table 3. For a supine position, Figure 6C indicates a significant amount of area shifting posteriorly with the tumor center lateral shift corroborating this directional shift, whereas Figure 6B indicates the surgeon's attempt to reduce this shift via a lateral decubitus position. A further advantage of the lateral decubitus position is that it makes use of the characteristics of the falx, which acts as a natural constraint on inter-hemispheric movement. In Figure 6B the area distribution and tumor center lateral shift direction suggest that rotation of the head was suitable but an insufficient

degree of tilt for shift minimization- the head was tilted in the direction opposite that needed for minimization. However, examination of the shift recovery sag vector in Figure 7 with respect to the placement of the craniotomy and in consideration of how the surgeon sits for surgery suggests that the tilt angle was chosen to permit easier access rather than for shift minimization.

The model optimized result in Figure 6D demonstrates three salient features of interest. First, especially with regards to the supine position yet also regarding the best shift orientation, a marked reduction in lateral shift of the tumor center can be seen. It is anticipated that the possibility of having the tumor stay under the point marked by the surgeon would be a considerable advantage when using image guidance that is not shift compensated. Second, examination of the perimeters of the area entering and leaving and of the craniotomy shows an intriguing degree of concentricity—i.e. the area distributions demonstrate a noticeable degree of symmetry. This concentricity likely corresponds to minimal lateral shift, but more cases would need to be analyzed to prove this conjecture. Third, a significant reduction in the area entering, a factor of a half compared to supine, means a lesser amount of healthy brain tissue falls into the resection cavity. In combination with the reduction in lateral shift of the tumor center, the reduced amount of area, distributed with the observed concentricity as a thin, fairly uniform band around the edges of the craniotomy, indicates a reduction of movement into the craniotomy of healthy tissue and hence a reduced potential need for retraction.

## 5. CONCLUSION

To our knowledge this is the first realization of an evaluative tool for surgical planning that attempts to optimize surgical approach by means of shift minimization. Currently shift minimization decisions depend mostly on the surgeon's expertise. The evaluative tool described here derives quantitative measures from a biomechanical model that accounts for gravitational forces and the effects of mannitol that can be used in a predictive sense to find an optimal orientation that minimizes brain shift. For a frontal lobe tumor, putting the patient in a lateral decubitus position on the side contralateral to the tumor has clear advantages over the supine position for reducing unfavorable brain shift and potentially reducing retractor usage. While preliminary in nature, this tool demonstrates an interesting clinical potential for aiding surgeons in orientating the patient.

## ACKNOWLEDGEMENTS

We wish to note our appreciation for the support of NIH-National Institute for Neurological Disorders and Stroke-Grant #R01 NS049251-01A1 for making this work possible.

## REFERENCES

- [1] T. Hartkens, D. L. G. Hill, A. D. Castellano-Smith, D. J. Hawkes, C. R. Maurer, A. J. Martin, W. A. Hall, H. Liu, and C. L. Truwit. Measurement and analysis of brain deformation during neurosurgery. *IEEE Transactions on Medical Imaging*, 22(1):82–92, January 2003.
- [2] C. Nimsy, O. Ganslandt, S. Cerny, P. Hastreiter, G. Greiner, and R. Fahlbusch. Quantification of, visualization of, and compensation for brain shift using intraoperative magnetic resonance imaging. *Neurosurgery*, 47(5):1070–1079, 2000.
- [3] A. Nabavi, P. M. Black, D. T. Gering, C. F. Westin, V. Mehta, R. S. Pergolizzi, M. Ferrant, S. K. Warfield, N. Hata, R. B. Schwartz, W. M. Wells, R. Kikinis, and F. A. Jolesz. Serial intraoperative magnetic resonance imaging of brain shift. *Neurosurgery*, 48(4):787–797, 2001.
- [4] D. W. Roberts, A. Hartov, F. E. Kennedy, M. I. Miga, and K. D. Paulsen. Intraoperative brain shift and deformation: A quantitative analysis of cortical displacement in 28 cases. *Neurosurgery*, 43(4):749–758, 1998.
- [5] K. Ha, P. Dumpuri, M. I. Miga, R. C. Thompson, 'Modeling surgical procedures to assist in understanding

surgical approach', *Medical Imaging 2007: Visualization and Image-Guided Procedures: Proc. of the SPIE*, (in press), 2007

[6] P. Dumpuri, R. C. Thompson, A. Cao, S. Ding, I. Garg, B. M. Dawant, and M. I. Miga, 'A fast efficient method to compensate for brain shift for tumor resection therapies measured between preoperative and postoperative tomograms', *IEEE Transactions on Biomedical Engineering*, (in press), 2009

[7] P. Dumpuri, R. C. Thompson, B. M. Dawant, A. Cao, M. I. Miga, 'An atlas-based method to compensate for brain shift: Preliminary results', *Medical Image Analysis*, Vol. 11, No. 2., pp.128-145, 2007

[8] M.A. Biot. General theory of three-dimensional consolidation. *J.Appl.Phys.*, 12:155–164, Feb 1941.

[9] M. I. Miga, K. D. Paulsen, J. M. Lemery, S. D. Eisner, A. Hartov, F. E. Kennedy, and D. W. Roberts. Model-updated image guidance: Initial clinical experiences with gravity-induced brain deformation. *IEEE Transactions on Medical Imaging*, 18(10):866–874, 1999.

[10] M. I. Miga, D. W. Roberts, A. Hartov, S. Eisner, J. Lemery, F. E. Kennedy, and K. D. Paulsen. Updated neuroimaging using intraoperative brain modeling and sparse data. *Stereotactic and Functional Neurosurgery*, 72(2-4):103–106, 1999.

[11] M. I. Miga, K. D. Paulsen, P. J. Hoopes, F. E. Kennedy, A. Hartov, and D. W. Roberts. In vivo quantification of a homogeneous brain deformation model for updating preoperative images during surgery. *IEEE Transactions on Biomedical Engineering*, 47(2):266–273, 2000.

[12] M. I. Miga, D. W. Roberts, F. E. Kennedy, L. A. Platenik, A. Hartov, K. E. Lunn, and K. D. Paulsen. Modeling of retraction and resection for intraoperative updating of images. *Neurosurgery*, 49(1):75–84, 2001.

[13] Nagashima T, Shirakuni T, Rapoport S: "A two-dimensional, finite element analysis of vasogenic brain edema," *Neurol Med Chir* 30:1-9, 1990

[14] M. I. Miga. *Development and quantification of a 3D brain deformation model for model-updated image-guided stereotactic neurosurgery*. PhD thesis, Thayer school of Engineering, Dartmouth College, september 1998.

[15] K.D. Paulsen, M.I. Miga, F.E. Kennedy, P.J. Hoopes, A. Hartov, and D.W. Roberts. A computational model for tracking subsurface tissue deformation during stereotactic neurosurgery. *IEEE Trans.Biomed.Eng*, 46(2):213–225, Feb 1999.

[16] M. I. Miga, K. D. Paulsen, F. E. Kennedy, P. J. Hoopes, A. Hartov, and D. W. Roberts. Initial *in-vivo* analysis of 3D heterogeneous brain computations for model-updated image-guided Neurosurgery. *Medical Image Computing and Computer-Assisted Intervention 1998: Lecture Notes in Computer Science*, Springer Verlag, New York, 1496, pp.743-752, 1998.